A novel ex vivo tracheobronchomalacia model for airway stent testing and in vivo model refinement

◉ Check for updates

Abhijit Mondal, PhD,[a,b] Gary A. Visner, DO,[c,d] Aditya K. Kaza, MD,[a,b] and Pierre E. Dupont, PhD[a,b]

ABSTRACT

Objectives: We sought to develop an ex vivo trachea model capable of producing mild, moderate, and severe tracheobronchomalacia for optimizing airway stent design. We also aimed to determine the amount of cartilage resection required for achieving different tracheobronchomalacia grades that can be used in animal models.

Methods: We developed an ex vivo trachea test system that enabled video-based measurement of internal cross-sectional area as intratracheal pressure was cyclically varied for peak negative pressures of 20 to 80 cm H_2O. Fresh ovine tracheas were induced with tracheobronchomalacia by single mid-anterior incision (n = 4), mid-anterior circumferential cartilage resection of 25% (n = 4), and 50% per cartilage ring (n = 4) along an approximately 3-cm length. Intact tracheas (n = 4) were used as control. All experimental tracheas were mounted and experimentally evaluated. In addition, helical stents of 2 different pitches (6 mm and 12 mm) and wire diameters (0.52 mm and 0.6 mm) were tested in tracheas with 25% (n = 3) and 50% (n = 3) circumferentially resected cartilage rings. The percentage collapse in tracheal cross-sectional area was calculated from the recorded video contours for each experiment.

Results: Ex vivo tracheas compromised by single incision and 25% and 50% circumferential cartilage resection produce tracheal collapse corresponding to clinical grades of mild, moderate, and severe tracheobronchomalacia, respectively. A single anterior cartilage incision produces saber-sheath type tracheobronchomalacia, whereas 25% and 50% circumferential cartilage resection produce circumferential tracheobronchomalacia. Stent testing enabled the selection of stent design parameters such that airway collapse associated with moderate and severe tracheobronchomalacia could be reduced to conform to, but not exceed, that of intact tracheas (12-mm pitch, 0.6-mm wire diameter).

Conclusions: The ex vivo trachea model is a robust platform that enables systematic study and treatment of different grades and morphologies of airway collapse and tracheobronchomalacia. It is a novel tool for optimization of stent design before advancing to in vivo animal models. (J Thorac Cardiovasc Surg 2023;166:679-87)
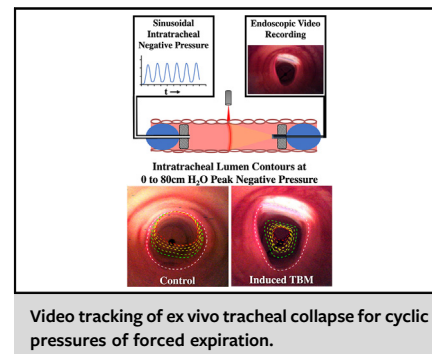
Video tracking of ex vivo tracheal collapse for cyclic pressures of forced expiration.

CENTRAL MESSAGE

An ex vivo tracheal testing platform is described that enables the refinement of TBM animal models and the rapid assessment of stent prototypes.

PERSPECTIVE

We address the need for a physiologically accurate and inexpensive platform for rapid stent testing and design optimization. The presented platform provides video-based airway collapse measurement for pressure cycles corresponding to forced expiration in intact tracheas and malacic tracheas with and without helical stent support. The platform also can be used to refine malacic airway animal models.

Tracheobronchomalacia (TBM) is the collapse of the large airway walls during expiration due to weakening of tracheal and mainstem bronchi segments in the supporting cartilage or the posterior membrane. When this weakening is limited only to the trachea, it is referred to as "tracheomalacia."

📎 ▶️ Scanning this QR code will take you to the table of contents to access supplementary information. To view the AATS Annual Meeting Webcast, see the URL next to the webcast thumbnail.

Narrowing of the airway during expiration impedes airflow resulting in poor gas exchange. TBM is a progressive airway disease, and although rare, it is observed in 13% of adults[1] and 30% of children[2] undergoing bronchoscopy. Symptoms leading to clinical presentation include dyspnea, episodic choking, chronic cough, hemoptysis, and periodic respiratory infections.[2] TBM can be diagnosed and assessed using an awake functional bronchoscopy, dynamic computed tomography, and pulmonary function studies.[3] The severity of the disease is graded based on the percentage reduction in the cross-sectional area (CSA) of the tracheal or bronchial lumen during forced expiration, deep breathing, Valsalva maneuver, or coughing. For diagnosis and assessment, dynamic bronchoscopy is considered the reference standard.[4] Dynamic computed tomography provides a noninvasive option that enables quantitative assessment by mapping the extent of the disease over the entire tracheobronchial tree.[5] The disease is graded as mild, moderate, or severe if the percentage reduction in CSA is between 51% and 75%, between 76% and 90%, or greater than 90%, respectively.[4] There is discussion on updating this scale range because studies have shown that even healthy patients have percentage collapse up to 70%.[6] TBM can be further classified based on the morphology of airway collapse corresponding to crescent, saber-sheath (or lateral), and circumferential.[3] Depending on the underlying disease, disease progression, and severity, TBM can be treated by continuous positive airway pressure, stenting, or surgery.[3]

Stenting is considered the preferred method of treating severe TBM in pediatric patients unable to manage with intermittent positive airway pressure ventilation.[3] In adults, severe TBM is treated surgically in carefully selected patients by tracheobronchoplasty or robotic tracheobronchoplasty.[7] In these patients, stents also serve as an intermediate airway support before surgery. Several stenting options are available in a mesh or tube design made from silicone, nitinol, polyester, composites,[8] and resorbable materials.[9-12] Complications associated with clinical use of silicone,[13] metal mesh,[14] or resorbable[10,15,16] internal stents are well reported and require chronic airway management after implantation. Although no stent design is ideal, solid silicone tubes are the preferred clinical option. Recently, external resorbable stents[9,11] show promise, but implantation requires complex surgery. Helical stents have generated some interest because they minimally affect mucus flow and

provide the potential for atraumatic removal.[17-20] Although most stents are designed as cylindrical tubes, noncircular profiles have also been developed that match the natural tracheal cross-sectional profile[17,21] to improve fitting and reduce stent migration.[22,23]

Because of the limitations and tradeoffs of existing devices, stent design continues to be an area of active research.[8] The design process is impeded, however, by limitations in the current mechanical testing methods and animal models available for refining and evaluating new stent concepts.

Initial design refinement is often performed using mechanical testing equipment to measure, for example, a stent's radial and bending stiffness.[24] Because the literature suggests that stents of high stiffness are more prone to the generation of granulation tissue as well as to tissue erosion,[8,25] these tests can be used to tune the design parameters of a new stent to match the stiffness of an existing stent that performs well with respect to these criteria.[21,24] A challenge of this approach, however, is that it is hard to understand how stiffness values relate to physiological conditions such as variation in airway CSA during specific breathing states. Furthermore, testing machines are typically designed for stents with circular cross-sections bringing into doubt tests performed on noncircular stent profiles.

After initial refinement of a stent design, animal testing provides the most reliable platform for assessing both short- and long-term in vivo performance.[26,27] In most animal models, TBM is surgically induced by partial or complete resection of tracheal cartilage rings while leaving intact the inner lumen of the trachea.[26] A significant challenge of these models is that the relationship between the fraction of cartilage removed and the grade of TBM is not known.

Ex vivo animal models represent an underused, but important middle ground between mechanical testing and animal models.[21,28,29] In this article, we present an ex vivo testing system that enables initial stent designs of any cross-sectional profile to be rapidly and inexpensively compared in terms of airway cross-section under physiologic dynamic loading conditions. This testing system also helps to improve in vivo testing by providing a means to relate the amount of cartilage resected to clinical definitions of mild, moderate, and severe TBM.

The system provides video-based measurement of tracheal CSA under cyclic pressure variations for peak negative pressures of 20 to 80 cm H_2O. This includes the intratracheal pressure range for TBM diagnosis by forced expiration.[30] In addition to determining the amount of cartilage resection corresponding to mild, moderate, and severe TBM, we also relate the degree of resection to the morphology of collapse. To demonstrate how the system can be used for stent design, we show how the design parameters of a helical stent can be selected to reduce the collapse experienced with severe and moderate TBM to that of a healthy trachea.

MATERIALS AND METHODS

Ex Vivo Testing System

The testing system is depicted in the schematic of Figure 1, *A*. The trachea is positioned over a warm water bath maintained at 37 °C and is irrigated every 5 to 10 minutes with warm phosphate-buffered saline. The tracheal lumen is sealed at both ends with latex balloons. The lumen of the balloon at the left end is connected to a pressure control circuit. The pressure circuit consists of a microprocessor-controlled (Arduino Uno, Bulk Construction Materials Initiative) linear actuator (Actuonix L12-EV3-100, Actuanix Motion Devices Inc) and pneumatic cylinder

(Bore diameter: 1.5 inch, stroke: 4 inch, Parker Hannifin Corp), which is programmed to produce intratracheal negative pressure oscillations of a specified magnitude and frequency based on pressure sensor measurements (#159905, Radnoti LLC). The actuator and cylinder were selected so that the model could produce oscillating intratracheal pressures with peak negative pressures of 20 to 80 cm H_2O and breathing rate of 20 breaths per minute. This fully covers the range reported for forced expiration as used in TBM diagnosis (average $\sim$30 cm H_2O, maximum $\sim$59 cm H_2O).[30]

The system was designed to apply oscillatory pressures for several reasons. First, initial testing demonstrated that tracheas maintained at static
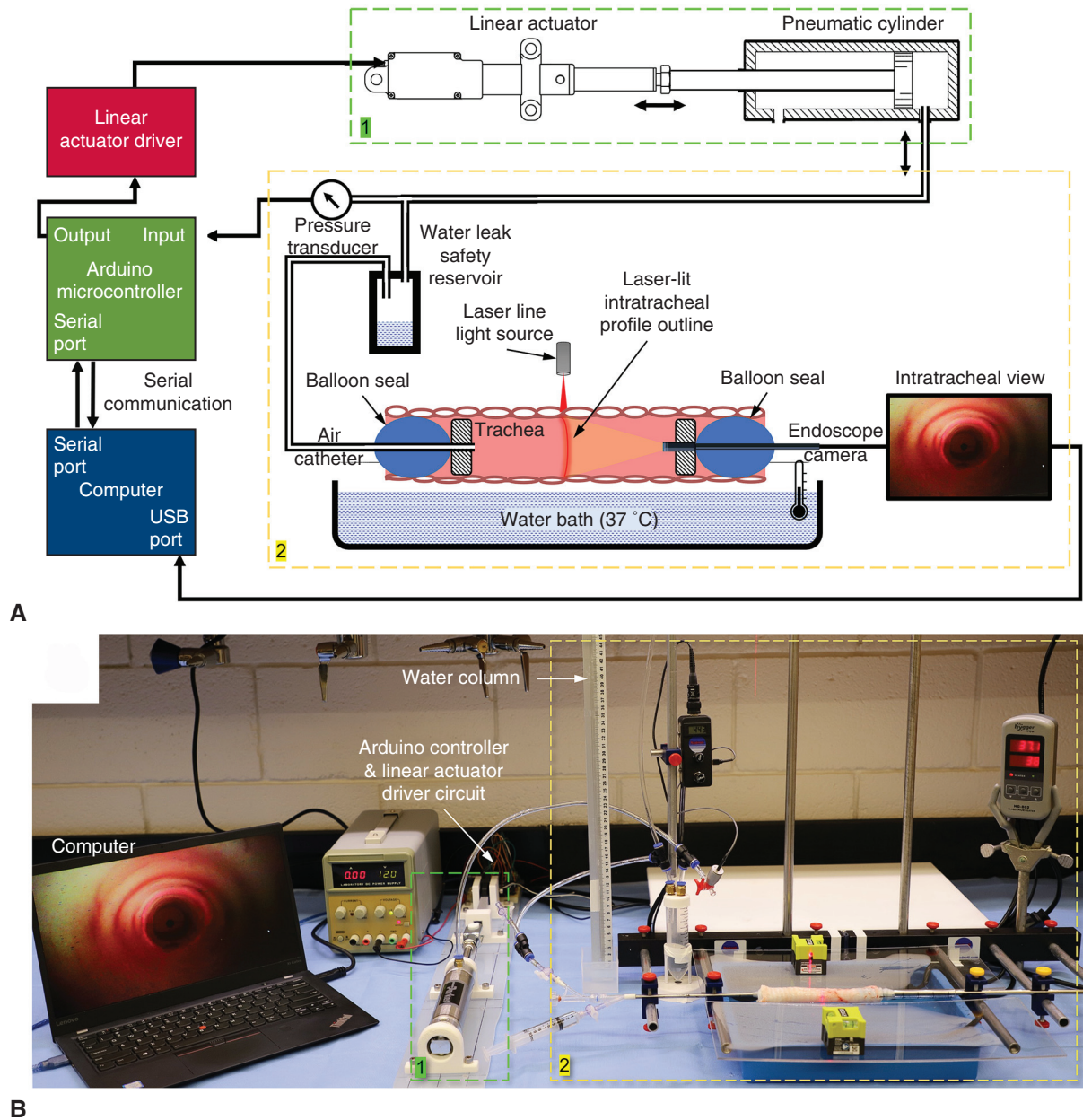

FIGURE 1. Ex vivo testing system. A, Schematic showing major components. The linear actuator coupled with pneumatic cylinder (in *dotted green box*) creates and controls the intratracheal negative pressure. The trachea is placed over a warm water bath and sealed with pressure inlet on *left* end and endoscope camera on *right* (in *dotted orange box*). Based on commands from the PC, a microcontroller uses pressure measurements to control the actuator so as to produce the desired oscillatory pressure. B, Testing system shown with an intact trachea.
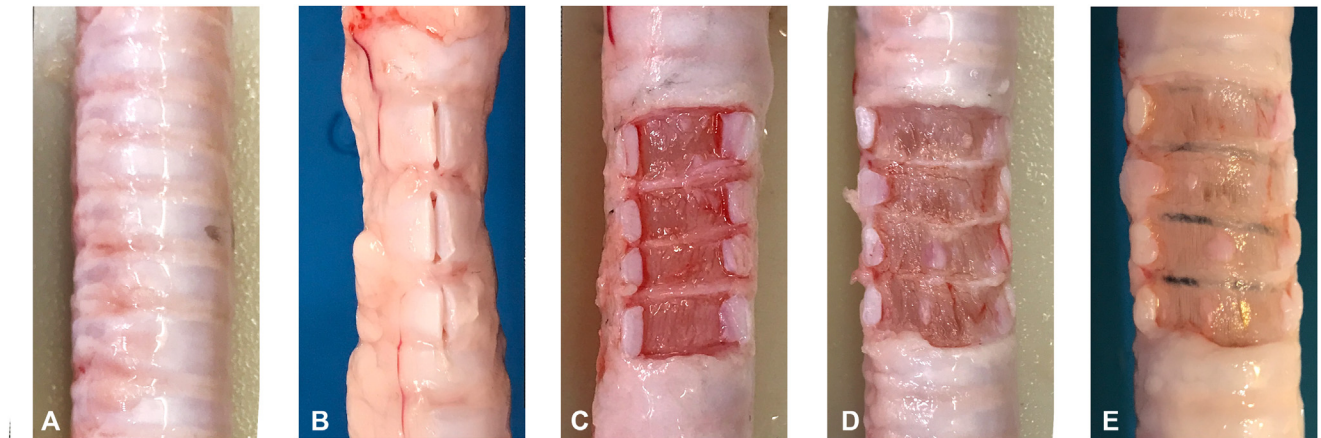
FIGURE 2. Mid-anterior views of experimental tracheas. A, Intact trachea. B-E, Tracheas with induced TBM (*iTBM*) showing selected region for incision or resection spanning approximately 3 cm. Different levels of TBM severity were induced by (B) single mid-anterior incision per cartilage, (C) 25% circumferential resection per cartilage, and (D) 50% circumferential resection per cartilage. E, An iTBM trachea (50% circumferentially resected cartilages) with an implanted helical stent.

negative pressures sometimes remained collapsed after the negative pressure was removed. By applying an oscillating pressure, it was possible to compare the cross-sections between cycles to confirm that no permanent deformation had occurred. In addition, cyclic loading made it possible to perform tissue preconditioning by running the system for an initial set of 6 cycles before data collection.[31-33] Finally, cyclic loading with a frequency matching the normal respiratory rate is more representative of physiologic conditions than static loading and provides information on the variation of the cross-section over a breathing cycle.

The microcontroller implements a feedback controller based on measured pressure to control actuator position and velocity. A safety reservoir is used to prevent any water from entering the cylinder or pressure transducer. Pressure commands are transferred from a PC by serial communication to the microcontroller, and experimental data are collected on the PC using the same communication channel.

Two laser line generators (ELL1750 Laser Cube, Ryobi Ltd) are positioned on opposite sides of the trachea to create a closed contour on the tracheal cross-section whose area is to be measured (Figure 1, *A*). The red laser light penetrates through the tracheal walls and is recorded to the PC using an endoscopic camera inserted through the lumen of the balloon at the right end. The experiments are performed without ambient light to maximize the contrast of the laser light.

Ex Vivo Tracheobronchomalacia Model

We procured fresh ovine tracheas (Research 89 Inc) from the cervical region of similar intratracheal lumen diameter of 14 to 16 mm for our study. All experiments were conducted within 36 hours of euthanasia and tissue harvest. The average cartilage width and inter-cartilage pitch of the study tracheas were measured.

Tracheas were prepared for 4 experimental conditions. The first condition served as control with intact tracheas (1). The other 3 conditions presented 3 levels of induced TBM by (2) cartilage single incision, (3) 25% radial cartilage resection (CR25), and (4) 50% radial cartilage resection (CR50) of approximately 3-cm length. Each trachea was stretched and fixed in position on a tissue board using clamps. The region of the mid-anterior wall of the cartilage to be incised or transected was marked. For creating single incision condition, the center of the mid-anterior wall of the cartilage was incised without puncturing through the submucosal and transitional epithelial layers. For creating cartilage resection conditions, the selected portion of the cartilage was transected and carefully detached from the trachea while preserving the submucosal and transitional epithelial layers. Figure 2 shows representative tracheas for the 4 experimental conditions.

Stent Evaluation

To demonstrate how the testing system could be used in stent design, 3 uncovered helical stent designs (Table 1) were evaluated in cyclic loading experiments. It has been shown that reduction of airway cross-section with this type of stent is composed of 2 components.[17,19] The first, which is typically the larger component, arises from the unsupported tissue between the coils bowing inward in a (helical) hourglass shape. The second component is due to radial compression of the helical coil. To assess the changes in airway reduction due to each of these components, the 3 stent designs listed next were tested. Stents 1 and 2 produce variation in the first component of collapse. They are made with the same wire diameter, but the pitch is doubled in stent 2, which doubles the length of unsupported tissue between the coils. Stents 2 and 3 produce variation in stent radial stiffness by using the same pitch, but different wire diameters.

Cyclic Loading Experiments

Each experimental trachea was mounted in the test system as described earlier. After fixing the trachea, tissue preconditioning was performed by applying 6 cycles at a magnitude of 20 cm H_2O. Subsequently, data were sequentially collected for 6 cycles per negative pressure magnitudes of 20, 30, 40, 50, 60, 70, and 80 cm H_2O using a period of 3 seconds (blue curve in Figure 3, *D*). Endoscopic videos were recorded for each experiment, and the videos were analyzed frame-by-frame to detect the laser-lit contour of the tracheal lumen (Figure 3, *E* and *F*). These data were processed to compute reduction in CSA as a function of time and to determine the maximum reduction associated with the peak pressure.

Table E1 lists all the experimental conditions investigated using the test system in the order the experiments were performed. A total of 12 ovine tracheas were used. The control tracheas were also used for the single incision experiments. The tracheas with CR25 and CR50 were also used to test the 3 NiTi helical stents (Table 1) whose lengths were sufficient to cover the entire TBM region (Figure 2, *E*).

TABLE 1. Stent specifications

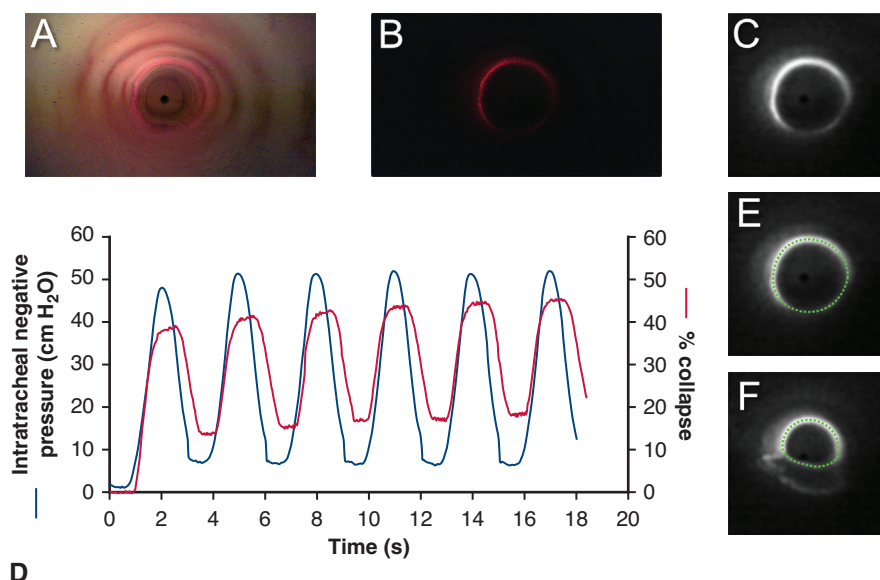| Stent	Helix pitch	Wire diameter
Stent 1	12 mm	0.6 mm
Stent 2	6 mm	0.6 mm
Stent 3	6 mm	0.52 mm

FIGURE 3. Tracheal lumen contour detection and determination of percentage change in tracheal CSA. A, Endoscopic view of tracheal lumen showing laser-lit contour in ambient light. B, Endoscopic view of (A) in darkened room. The laser-lit contour is easily distinguishable. C, Cropped and processed gray-scale image enhances the laser-lit tracheal-lumen contour (in *white*). D, Plot showing intratracheal negative pressure and percentage collapse in tracheal CSA with time. Note time synchronization of plots is approximate. E, Automated tracheal lumen contour tracking (*dotted green*) using snake contour method at zero intratracheal pressure. F, Detected contour at negative 50 cm H_2O.

Data and Statistical Analysis

A total of 238 endoscopic video clips corresponding to the 10 experimental conditions were recorded and analyzed. Automated tracheal lumen contour detection was performed frame-by-frame using MATLAB 2019 (Mathworks). The process involved considering only the red channel of the color image. This was cropped from the side and contrast enhanced and filtered using a Gaussian filter (Figure 3, *C*). The initial contour was set by detecting the peak pixel intensity along the radial direction from the center of the image. This was used as an initial guess for the Snake Contour method[34,35] to detect the final intratracheal contour (Figure 3, *E* and *F*). Video 1 shows the intratracheal contour and its calculated CSA in real-time for the experimental condition in Figure 3.

CSA of the closed contour is used to calculate the percentage collapse in the trachea at any given time, *t*:

$$\%collapse(t) = \frac{CSA(0) - CSA(t)}{CSA(0)} \times 100$$

For each experiment, the percentage collapse was plotted against time (Figure 3, *D*) for all 6 cycles. The maxima were tabulated, and the percentage collapse corresponding to the pressure value closest to the desired peak pressure value was selected.

To assess the significance of difference in percentage collapse between the experimental tracheas (control, cartilage single incision, CR25, and CR50), 1-way analysis of variance tests (anova1.m, MATLAB 2019) were performed in MATLAB 2019. Student *t* tests (ttest2.m, MATLAB 2019) were performed pairwise for experimental conditions involving stents (stents 1, 2, and 3). Statistical tests were performed separately for each pressure value. The maximum or minimum *P* value has been reported to show significant or no significant difference, respectively.

RESULTS

Severity of Bronchomalacia Versus Amount of Cartilage Resected

The average cartilage ring width of the tested tracheas was 4.7 mm ± 1.0 mm (range, 3.3-7.4 mm). Resection of approximately 25% and approximately 50% corresponded to removing cartilage ring lengths of 15 mm ± 2 mm (range, 13-19 mm) and 24 mm ± 2 mm (range, 21-26 mm), respectively. The average center-to-center spacing between cartilage rings was 6.5 mm ± 1.3 mm (range, 4.8-8.8 mm). The number of rings incised or resected was 4.1 ± 0.6 (range, 3-5).

Figure 4 summarizes the results from the experiments conducted on intact and malacic tracheas. For the control tracheas, the percentage reduction in CSA varied between 27% ± 4% at 20 cm H_2O and 58% ± 2% at 80 cm H_2O. Although collapse exceeded 50%, it only did so at pressures exceeding those of forced expiration, and so this behavior would not be classified as malacic.
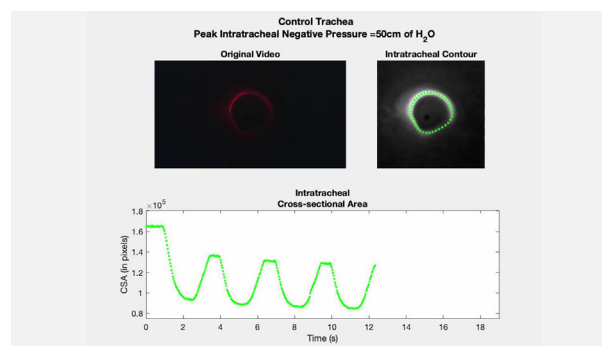
VIDEO 1. Intratracheal CSA calculation using automated video analysis in control trachea under cyclic peak negative intratracheal pressure of 50 cm of H_2O. Video available at: https://www.jtcvs.org/article/S0022-5223(23)00333-1/fulltext.

A single incision through the cartilage, however, was sufficient to produce airway reduction greater than 50% for pressures of 30 cm H_2O and higher. For a negative pressure peak of 80 cm H_2O, percentage CSA reduction just exceeds 70% indicating that a single incision provides a good model for mild TBM.

For CR25, lumen percentage CSA reduction exceeds 75% at 30 cm H_2O and exceeds 90% area reduction between 70 and 80 cm H_2O. Consequently, the CR25 model corresponds to moderate TBM for most of the pressure range associated with forced exhalation.

In tracheas with 50% circumferential cartilage resection, the percentage collapse ranges from 73% $\pm$ 4% to 99% $\pm$ 1% as negative pressure was raised from 20 cm to 80 cm, respectively. This amount of resection produces a model of moderate TBM for negative pressures up to 40 cm H_2O and severe TBM at higher negative pressures.

One-way analysis of variance tests performed for peak percentage collapse of the 4 experimental groups for each intratracheal pressure value showed significant difference ($P < 1.3 \times 10^{-8}$).

Stent Testing Enables Tuning of Design Parameters

Video 2 shows the real-time collapse of intratracheal lumens in unsupported and stent-supported induced TBM trachea (CR50) under cyclic intratracheal peak pressure of 80 cm of H_2O. Figure 5 compares the collapse of the stented tracheas with CR25 and CR50 resection to that of the intact control tracheas. Comparing the stents with different pitches, corresponding to different unsupported lengths of tissue between the coils, it is observed that the stents with a 6-mm pitch reduce airway collapse substantially more than what is observed in a control trachea (1-tail t test: $P < .008$). In contrast, the stent with a 12-mm pitch produces an area reduction less than but still close to that of the control trachea (2-tail t test: $P > .06$ for <70 cm H_2O pressure). This suggests that the stents with a 6-mm pitch are overly stiff.

In comparing stents 2 and 3, which both have a 6-mm pitch, stent 2 uses the larger wire diameter and so is radially stiffer. The corresponding experimental result is that it experiences slightly less area reduction than stent 3 (2-tail t test: $P > .05$). Taken together, these tests suggest that
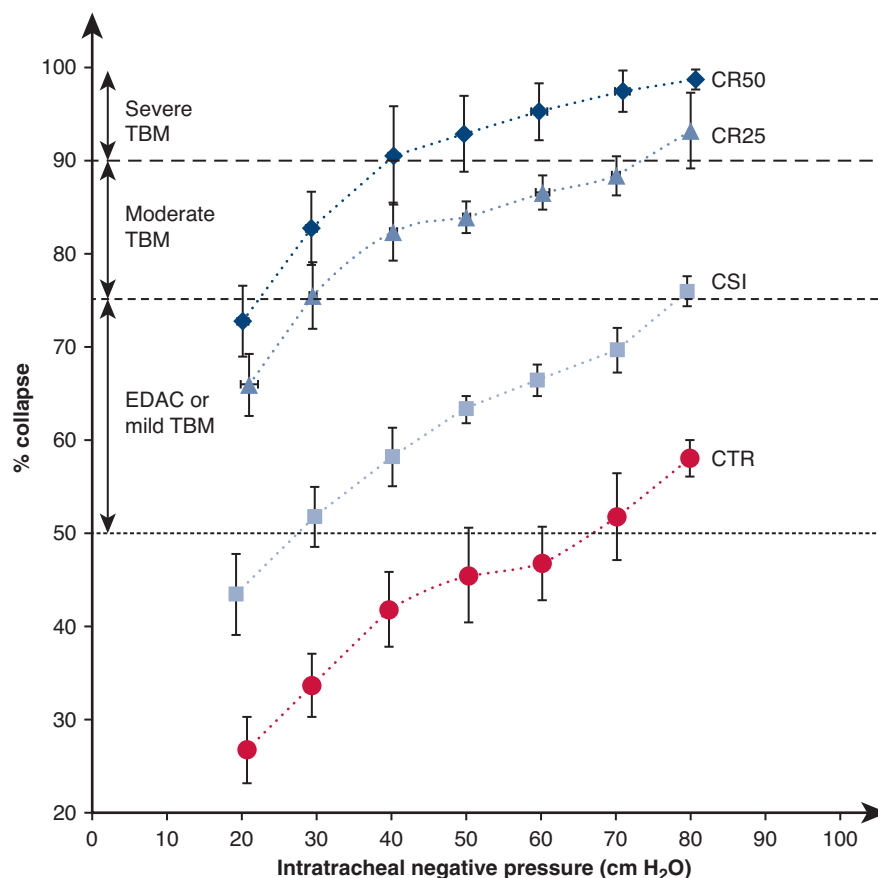

FIGURE 4. Percentage reduction in tracheal cross-section as a function of peak negative pressure. Ranges of area reduction associated with mild (51%-75%), moderate (76%-90%), and severe (>91%) are noted. The percentage collapse in the 4 experimental groups for each intratracheal pressure value had statistically significant differences (1-way analysis of variance: $P < 1.3 \times 10^{-8}$). *TBM*, Tracheobronchomalacia; *CR50*, 50% cartilage resection; *CR25*, 25% cartilage resection; *EDAC*, excessive dynamic airway collapse; *CSI*, single incision per cartilage; *CTR*, control.
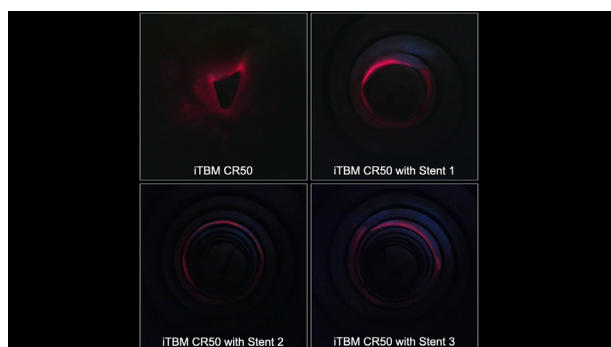
VIDEO 2. Endoscopic videos of LASER-lit tracheal lumen in unsupported and stent-supported induced TBM trachea under cyclic peak negative intratracheal pressure of 80 cm of H_2O. Video available at: https://www.jtcvs.org/article/S0022-5223(23)00333-1/fulltext.

further design optimizations should consider smaller wire diameters with a helical pitch of approximately 12 mm.

Airway Collapse Morphologies in Intact and Induced Tracheobronchomalacia Tracheas

As shown in Figure 6, three different morphologies of cross-sectional contraction were observed during testing. In the control trachea, most of the contraction, as expected,
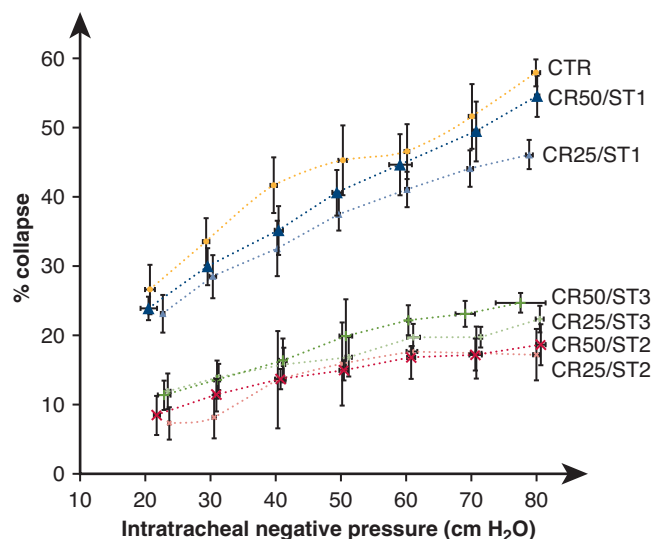

FIGURE 5. Stent performance in treating moderate and severe iTBM. The percentage collapse in tracheal CSA versus intratracheal negative pressure plots in intact trachea (*yellow*) and iTBM tracheas treated with 3 helical stents of different pitch and wire diameters (stent 1: P12 mm, WD 0.6 mm, stent 2: P6 mm WD 0.6 mm and stent 3: P6 mm WD 0.52 mm). Each stent was tested in tracheas with 25% (*lighter shade*, CR25) and 50% (*darker shade*, CR50) cartilage removed. Plots indicate that 12-mm pitch was sufficient to produce collapse close to that of an intact trachea (2-tail *t* test: *P* > .06 for <70 cm H_2O pressure). Stents with lower pitch (P6 mm in stents 2 and 3) are overly stiff and reduce tracheal collapse significantly more than that of the control trachea (1-tail *t* test: *P* < .01). *CTR*, Control; *CR50*, 50% cartilage resection; *ST*, stent; *CR25*, 25% cartilage resection; *P*, pitch.

occurs in the posterior membrane of the trachea (Figure 6, A). Although not malacic, the shape is like the crescent type of TBM. In tracheas with a single incision, a significant lateral component of contraction is observed that is comparable to the saber-sheath type of TBM (Figure 6, B). In malacic tracheas with 25% to 50%, collapse occurs in all directions (Figure 6, C and D) mimicking the circumferential type of TBM. Video 3 shows the intratracheal lumens in real-time from the 4 experimental tracheas under cyclic peak negative intratracheal pressure of 80 cm of H_2O.

DISCUSSION

Our results demonstrate that ex vivo testing systems can provide a valuable approach for performing stent design optimization and refining in vivo animal models. Designing the testing system to apply cyclic pressures provides several benefits. First, the observed temporal variation in tracheal cross-section can be more closely related to physiologic variation over the breathing cycle. Second, it provides a means to precondition the tissue before data collection. Third, it avoids the permanent airway collapse associated with maintained static loading that was observed during system development.

When applied to stent design, the testing system enables rapid comparison of design alternatives in which critical parameters are varied. In the examples considered here, helical stents with different wire diameters and helical pitches were considered. The system provided the means to compare the pressure-dependent airway collapse of stented malacic tracheas with that of intact control tracheas. In this way, stent designs can be tuned to provide sufficient support without being overly stiff, which can potentially increase granulation tissue or cause tissue erosion.[8,25]

In addition to stent design, the ex vivo testing system provides a means of interpreting animal models for TBM. For example, using the TBM model in which a portion of each cartilage ring is removed (Figure 4), we were able to relate the severity of the TBM with the amount removed. A single cartilage incision produced mild TBM (50%-75% area reduction) for pressures associated with forced exhalation. Likewise, removing 25% of the cartilage rings produced moderate TBM (76%-90% area reduction) while removing 50% of the rings produced moderate to severe TBM (>91% area reduction). Furthermore, the intact control tracheas exhibited mild TBM for negative intratracheal pressures of 70 cm H_2O and above. Although these pressures exceed those typically associated with forced exhalation,[30] they are well below those of coughing and support the ongoing controversy of assuming 50% area reduction is indicative of TBM.[4]

The results of this study can aid in refining the design of animal studies, for example, cartilage resection model of TBM. One could design in vivo experiments in which a specific desired degree of TBM is achieved. Without this knowledge, the temptation is to remove a large amount of cartilage to ensure that TBM occurs. This typically results in such
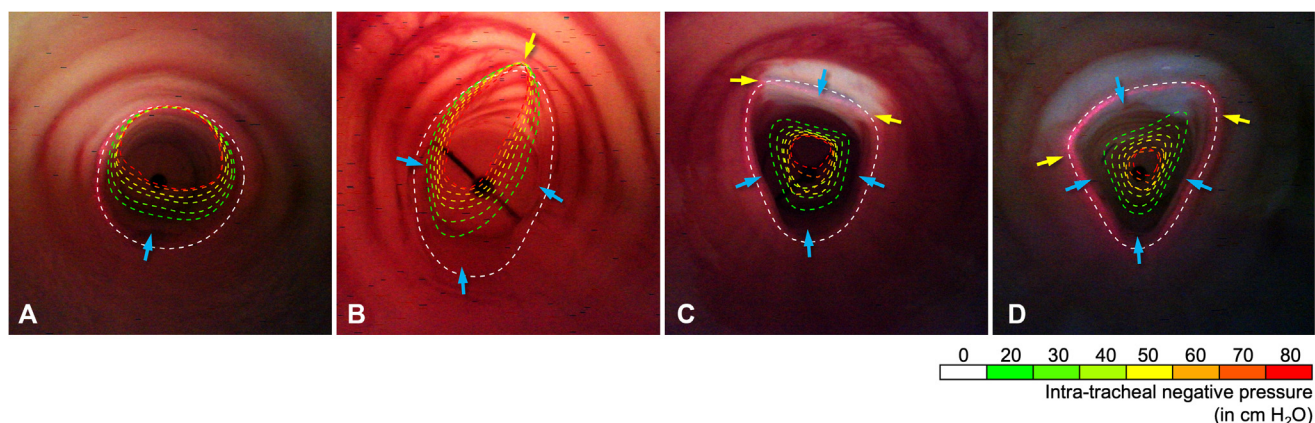
FIGURE 6. Tracheal collapse morphologies in control and different modes of iTBM. *Dotted lines* present the tracheal-lumen's profile at intratracheal negative pressure from 0 to 80 cm H_2O in (A) intact trachea, (B) trachea with single incision per cartilage, (C) trachea with 25% circumferential resection per cartilage, and (D) trachea with 50% circumferential resection per cartilage. Point or region of cartilage incision/resection is indicated using *yellow arrows* in the malacic tracheas (B-D). Directions of collapse are indicated with *blue arrows*. In intact trachea, the collapse occurs from posterior membranous tracheal wall (A) as expected during dynamic airway collapse. A single mid-anterior cartilage incision creates a hinge point, causing collapse to occur more laterally (B) as in the saber-sheath type TBM. Partial resection of cartilage rings causes the tracheal wall to collapse from all directions as in circumferential TBM.

severe TBM that the animal cannot survive without significant airway support. Such a model precludes the inclusion of unstented controls, causes animal loss and suffering in the case of stent migration or malfunction, and is not representative of the majority of patients with TBM.

Study Limitations

As in existing animal models, our model relies on inducing TBM by creating airway-wall weakness through removal of cartilage segments. This weakened airway-wall does not necessarily match the biomechanical properties of TBM airways. Acquiring or creating such TBM tracheas remains a challenge.

This study focused on inducing TBM by weakening or injuring the anterior aspect of the tracheal walls that present only circumferential and saber-sheath TBM morphologies. Collapse of posterior tracheal aspects creates excessive
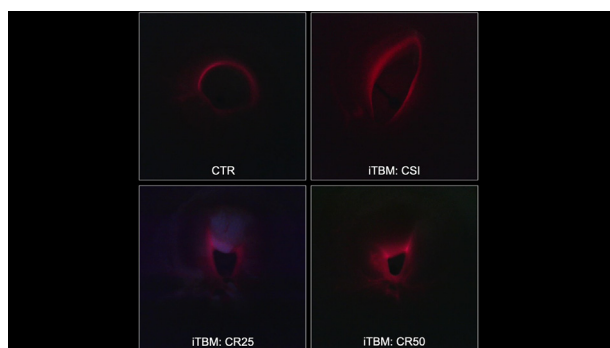
dynamic airway collapse or crescent-type TBM, the most common morphologies presented in the clinic. We plan future studies to quantify posterior collapse by injury to the posterior tracheal aspect.[29]

Because the testing system uses ex vivo tissue, the measured cross-sectional collapse will differ from what would be measured in vivo for the same transmural pressure. This will be due to changes in the mechanical properties of the tissue and to the changes in boundary conditions associated with excising the trachea from the surrounding tissues. Although it is anticipated that the ex vivo results will approximate those of in vivo testing, future studies are needed to compare ex vivo and in vivo testing results. Such comparisons will improve our ability to interpret ex vivo results, that is, to understand if ex vivo testing tends to overestimate or underestimate airway CSA as a function of pressure.

The testing system was designed to apply oscillating pressures to approximate physiologic variations in airway cross-section during forced breathing while also enabling tissue preconditioning. To provide a more accurate representation of the respiratory cycle, the system could be enhanced to expand the pressure cycles that can be produced. In particular, to include inspiration, the system could be modified to vary pressure between a peak negative value and a peak positive value. A peak positive pressure of 10 to 20 cm H_2O would be sufficient.[30] Simulated coughing is also of interest, but this would likely require adding a separate cough generator as described by Freitag and colleagues[21] to generate a rapid pressure pulse.

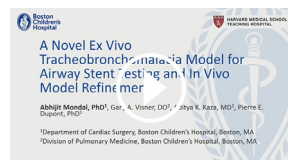**VIDEO 3.** Endoscopic videos of LASER-lit tracheal lumen in control and induced TBM tracheas (cartilage single incision, CR25, and CR50) under cyclic peak negative intratracheal pressure of 80 cm of H_2O. Video available at: https://www.jtcvs.org/article/S0022-5223(23)00333-1/fulltext.

CONCLUSIONS

This study demonstrates how an ex vivo tracheal testing system can be used to interpret and refine TBM animal

models. It also provides a cost-effective and time-efficient complement to mechanical and in vivo testing of stent prototypes.

Webcast 🔊

You can watch a Webcast of this AATS meeting presentation by going to: https://www.aats.org/resources/a-novel-ex-vivo-tracheobronchomalcia-model-for-airway-stent-testing-and-design-optimization.

A Novel Ex Vivo
Tracheobronchomalacia Model for
Airway Stent Testing and In Vivo
Model Refinement

Abhijit Mondal, PhD¹, Gar, A. Visner, DO², Aditya K. Kaza, MD¹, Pierre E. Dupont, PhD¹

¹Department of Cardiac Surgery, Boston Children's Hospital, Boston, MA
²Division of Pulmonary Medicine, Boston Children's Hospital, Boston, MA

Conflict of Interest Statement

P.E.D. and A.K.K are inventors on a US patent application held by Boston Children's Hospital that covers helical stent technology. All other authors reported no conflicts of interest.

The *Journal* policy requires editors and reviewers to disclose conflicts of interest and to decline handling or reviewing manuscripts for which they may have a conflict of interest. The editors and reviewers of this article have no conflicts of interest.

References

1. Ikeda S, Hanawa T, Konishi T, Adachi M, Sawai S, Chiba W, et al. Diagnosis, incidence, clinicopathology and surgical treatment of acquired tracheobronchomalacia. *Nihon Kyobu Shikkan Gakkai Zasshi*. 1992;30:1028-35.
2. Carden KA, Boiselle PM, Waltz DA, Ernst A. Tracheomalacia and tracheobronchomalacia in children and adults: an in-depth review. *Chest*. 2005;127:984-1005.
3. Murgu S, Colt H. Tracheobronchomalacia and excessive dynamic airway collapse. *Clin Chest Med*. 2013;34:527-55.
4. Majid A, Gaurav K, Sanchez JM, Berger RL, Folch E, Fernandez-Bussy S, et al. Evaluation of tracheobronchomalacia by dynamic flexible bronchoscopy. A pilot study. *Ann Am Thorac Soc*. 2014;11:951-5.
5. Aslam A, Cardenas JDL, Morrison RJ, Lagisetty KH, Litmanovich D, Sella EC, et al. Tracheobronchomalacia and excessive dynamic airway collapse: current concepts and future directions. *Radiographics*. 2022;42:1012-27.
6. Boiselle PM, O'Donnell CR, Bankier AA, Ernst A, Millet ME, Potemkin A, et al. Tracheal collapsibility in healthy volunteers during forced expiration: assessment with multidetector CT. *Radiology*. 2009;252:255-62.
7. Lazzaro RS, Bahroloomi D, Wasserman GA, Patton BD. Robotic tracheobronchoplasty: technique. *Operat Tech Thorac Cardiovasc Surg*. 2022;27:218-26.
8. Folch E, Keyes C. Airway stents. *Ann Cardiothorac Surg*. 2018;7:273-83.
9. Morrison RJ, Hollister SJ, Niedner MF, Mahani MG, Park AH, Mehta DK, et al. Mitigation of tracheobronchomalacia with 3D-printed personalized medical devices in pediatric patients. *Sci Transl Med*. 2015;7:285ra264.
10. Sztano B, Kiss G, Marai K, Racz G, Szegesdi I, Racz K, et al. Biodegradable airway stents in infants - potential life-threatening pitfalls. *Int J Pediatr Otorhinolaryngol*. 2016;91:86-9.
11. Zopf DA, Flanagan CL, Wheeler M, Hollister SJ, Green GE. Treatment of severe porcine tracheomalacia with a 3-dimensionally printed, bioresorbable, external airway splint. *JAMA Otolaryngol Head Neck Surg*. 2014;140:66-71.
12. Dutau H, Musani AI, Laroumagne S, Darwiche K, Freitag L, Astoul P. Biodegradable airway stents - bench to bedside: a comprehensive review. *Respiration*. 2015;90:512-21.
13. Bolliger CT, Probst R, Tschopp K, Soler M, Perruchoud AP. Silicone stents in the management of inoperable tracheobronchial stenoses. Indications and limitations. *Chest*. 1993;104:1653-9.
14. FDA. Public health notification: complications from metallic tracheal stents in patients with benign airway disorders. Accessed October 15, 2015. http://www.fda.gov/ MedicalDevices/Safety/AlertsandNotices/PublicHealthNotifications/ucm062 115.htm
15. Sztano B, Rovo L. Response to the letter to the editor "Biodegradable airway stents in infants - potential life-threating pitfalls". *Int J Pediatr Otorhinolaryngol*. 2017;98:175-6.
16. Vondrys D, Anton-Pacheco Sanchez J. Letter to the editor regarding "Biodegradable airway stents in infants - potential life-threatening pitfalls". *Int J Pediatr Otorhinolaryngol*. 2017;98:174.
17. Mencattelli M, Mondal A, Miale R, Van Story D, Peine J, Li Y, et al. In vivo molding of airway stents. *Adv Funct Mater*. 2021;31:2010525.
18. Mondal A, Ha J, Jo VY, Wu FY, Kaza AK, Dupont PE. Preclinical evaluation of a pediatric airway stent for tracheobronchomalacia. *J Thorac Cardiovasc Surg*. 2020;161:e51-60.
19. Ha J, Mondal A, Zhao Z, Kaza AK, Dupont PE. Pediatric airway stent designed to facilitate mucus transport and atraumatic removal. *IEEE Trans Biomed Eng*. 2020;67:177-84.
20. Serrano-Casorran C, Lopez-Minguez S, Rodriguez-Zapater S, Bonastre C, Guirola JA, De Gregorio MA. A new airway spiral stent designed to maintain airway architecture with an atraumatic removal after full epithelization-research of feasibility and viability in canine patients with tracheomalacia. *Pediatr Pulmonol*. 2020;55:1757-64.
21. Freitag L, Eicker R, Linz B, Greschuchna D. Theoretical and experimental basis for the development of a dynamic airway stent. *Eur Respir J*. 1994;7:2038-45.
22. Jung HS, Chae G, Kim JH, Park CY, Lim S, Park SE, et al. The mechanical characteristics and performance evaluation of a newly developed silicone airway stent (GINA stent). *Sci Rep*. 2021;11:7958.
23. Ryu YJ, Kim H, Yu CM, Choi JC, Kwon YS, Kim J, et al. Comparison of natural and Dumon airway stents for the management of benign tracheobronchial stenoses. *Respirology*. 2006;11:748-54.
24. Freitag L, Eicker K, Donovan TJ, Dimov D. Mechanical properties of airway stents. *J Bronchol Interv Pulmonol*. 1995;2:270-8.
25. Hu HC, Liu YH, Wu YC, Hsieh MJ, Chao YK, Wu CY, et al. Granulation tissue formation following Dumon airway stenting: the influence of stent diameter. *Thorac Cardiovasc Surg*. 2011;59:163-8.
26. Tsukada H, O'Donnell CR, Garland R, Herth F, Decamp M, Ernst A. A novel animal model for hyperdynamic airway collapse. *Chest*. 2010;138:1322-6.
27. Vinograd I, Filler RM, England SJ, Smith C, Poenaru D, Bahoric A, et al. Tracheomalacia: an experimental animal model for a new surgical approach. *J Surg Res*. 1987;42:597-604.
28. Kaye R, Goldstein T, Aronowitz D, Grande DA, Zeltsman D, Smith LP. Ex vivo tracheomalacia model with 3D-printed external tracheal splint. *Laryngoscope*. 2017;127:950-5.
29. Cao A, Swami P, Kaye R, Goldstein T, Grande DA, Smith LP. An ex vivo model of posterior tracheomalacia with evaluation of potential treatment modalities. Laryngoscope. Published online September 8, 2022. https://doi.org/10.1002/lary.30383
30. Loring SH, O'Donnell CR, Feller-Kopman DJ, Ernst A. Central airway mechanics and flow limitation in acquired tracheobronchomalacia. *Chest*. 2007;131:1118-24.
31. Fung YC. Biomechanics: Mechanical Properties of Living Tissues. Springer; 1981.
32. Safshekan F, Tafazzoli-Shadpour M, Abdouss M, Shadmehr MB. Mechanical characterization and constitutive modeling of human trachea: age and gender dependency. *Materials*. 2016;9:456.
33. Bagnoli P, Acocella F, Di Giancamillo M, Fumero R, Costantino ML. Finite element analysis of the mechanical behavior of preterm lamb tracheal bifurcation during total liquid ventilation. *J Biomech*. 2013;46:462-9.
34. Kumar R. Snakes: active contour models. MATLAB central file exchange. Accessed July 10, 2022. https://www.mathworks.com/matlabcentral/fileexchange/28109-snakes-active-contour-models
35. Xu C, Prince JL. Snakes, shapes, and gradient vector flow. *IEEE Trans Image Process*. 1998;7:359-69.

Key Words: airway stents, ex vivo model, stent testing, tracheobronchomalacia, tracheomalacia

TABLE E1. Experimental conditions

Stent no.	Group	Experimental condition	n
1	CTR	Intact trachea (control)	4
2	CSI	Trachea with single incision per cartilage	4
3	CR25	Trachea with 25% radially resected cartilage	4
4	CR50	Trachea with 50% radially resected cartilage	4
5	CR25/ST1	25% cartilage resected trachea treated with stent 1	3
6	CR25/ST2	25% cartilage resected trachea treated with stent 2	3
7	CR25/ST3	25% cartilage resected trachea treated with stent 3	3
8	CR50/ST1	50% cartilage resected trachea treated with stent 1	3
9	CR50/ST2	50% cartilage resected trachea treated with stent 2	3
10	CR50/ST3	50% cartilage resected trachea treated with stent 3	3

CTR, Control; *CSI*, single incision per cartilage; *ST*, stent.